Tristetraprolin Down-regulates Interleukin-8 and Vascular Endothelial Growth Factor in Malignant Glioma Cells

Esther Suswam,[1] Yanyan Li,[1,7] Xiaowen Zhang,[1,7] G. Yancey Gillespie,[4,6] Xuelin Li,[1,7] John J. Shacka,[5,7] Liang Lu,[1,7] Lei Zheng,[1,7] and Peter H. King[1,2,3,7]

Departments of [1]Neurology, [2]Genetics, [3]Physiology and Biophysics, [4]Cell Biology, [5]Pathology, and [6]Surgery, University of Alabama and [7]Birmingham Veterans Affairs Medical Center, Birmingham, Alabama

Abstract

Malignant gliomas are highly aggressive tumors of the central nervous system that rely on production of growth factors for tumor progression. Vascular endothelial growth factor (VEGF), interleukin-8 (IL-8), and tumor necrosis factor-α, for example, are up-regulated in these tumors to promote angiogenesis and proliferation. RNA stability, mediated through adenine and uridine-rich elements (ARE) in the 3′ untranslated region, is a critical control point for regulating these growth factors. RNA half-life is predominantly governed by a balance between stabilizing and destabilizing factors that bind to ARE. We have previously shown that the stabilizing factor HuR is overexpressed in malignant gliomas and linked to RNA stabilization of angiogenic growth factors. Here, we report that the destabilizing factor tristetraprolin (TTP) is also ubiquitously expressed in primary malignant glioma tissues and cell lines. In contrast to benign astrogliotic tissues, however, the protein was hyperphosphorylated, with evidence implicating the p38/mitogen-activated protein kinase (MAPK) pathway. Conditional overexpression of TTP as a transgene in malignant glioma cells led to RNA destabilization of IL-8 and VEGF and down-regulation of protein production. Analysis of *in vivo* RNA binding indicated a shift of mRNA toward ectopic TTP and away from endogenous HuR. This biochemical phenotype was associated with a decrease in cell proliferation, loss of cell viability, and apoptosis. We postulate that hyperphosphorylation of TTP via p38/MAPK promotes progression of malignant gliomas by negatively regulating its RNA destabilizing function. [Cancer Res 2008;68(3):674–82]

Introduction

Vascular endothelial growth factor (VEGF) and interleukin-8 (IL-8) promote proliferation and angiogenesis within malignant glioma tumors through autocrine or paracrine pathways (1–3). Expression of these angiogenic growth factors correlates with tumor grade and vascularity, and a number of extracellular signals, including hypoxia and cytokine exposure, serve as potent inducers of gene expression (2, 3). Strong expression of IL-8 and VEGF, for example, is observed in hypoxic/anoxic pseudopallisading cells within glioblastoma multiforme (GBM). Major determinants of IL-8 and VEGF RNA induction reside at transcriptional and posttranscriptional levels of gene regulation, working in concert to provide sustained RNA levels for protein translation (3, 4). RNA stabilization, mediated through adenine and uridine-rich elements (ARE) in the 3′ untranslated region (UTR), represents a major component of posttranscriptional regulation in malignant glioma and other tumors (4, 5). We have shown that HuR, an mRNA-binding protein (RBP) linked to ARE-mediated RNA stabilization, is overexpressed in malignant glioma, leading to up-regulation of VEGF, IL-8, and tumor necrosis factor-α (TNF-α) transcripts (6, 7). This level of gene regulation, however, reflects a balance between factors, such as HuR and those associated with destabilization, like tristetraprolin (TTP), butyrate response factor-1, KH-type splicing regulatory protein (KSRP), and adenine and uridine-rich RNA binding factor 1 (AUF1). Little is known about RNA destabilizing factors in malignant glioma, but based on our previous work and that of other investigators, we hypothesized that they would be suppressed. Here, we investigate the RNA destabilizer TTP in malignant glioma and find that this RBP is universally expressed in tumor and control tissues, but is hyperphosphorylated in the former to a state that has been associated with reduced function. Ectopic overexpression in glioma cells, however, leads to RNA destabilization of IL-8 and VEGF and an adverse effect on tumor cell proliferation and viability. These findings, in conjunction with our previous reports with HuR, suggest that the status of angiogenic factor mRNA stability is directly related to a balance between stabilizing and destabilizing RBPs, which in turn has a direct effect on tumor growth.

Materials and Methods

DNA constructs, cell culture, and transfection. Human TTP cDNA was the generous gift of Dr. Chris Moroni. The coding region was PCR amplified to create a FLAG epitope at the N terminus using the following primers: upstream, 5′-TCAAGCTTGCGGCCGCATGGACTACAAGGACGACGATGACAAGGATCTGACTGCCATCTACG-3′ and downstream, 5′-TAGACCTTGATATC TCACTCAGAAACAGAGATGC-3′. The PCR product was digested with *Not*1 and *Eco*RV, cloned into the pTRE2-hyg plasmid (Clontech) and verified by sequencing. U87MG, U118MG, U138MG, M059K human glioma cell lines were purchased from the American Type Culture Collection. U251MG, U105MG, and D37MG human glioma cell lines were a kind gift from Dr. Darell D. Bigner (Duke University). The SNB19 human glioma cell line was a kind gift from Dr. Richard S. Morrison (University of Washington), and U251MG tet-on cells were from Dr. Erwin Van Meir (Emory University). Plasmid transfection and clone selection are described elsewhere (7). For cytokine stimulation, cells were treated with TNF-α (R&D Systems) at 10 ng/mL for 24 h.

Western analysis, ELISA, and antibodies. For Western analysis, tumor tissues were provided by the UAB Brain Tumor Specialized Programs of Research Excellence tissue core facility. Protein was extracted in the presence of protease inhibitors and sodium orthovanadate using the M-PER or T-PER kit (Pierce Endogen). Sixty micrograms of extract were resolved on a 10% SDS-polyacrylamide and blotted. For dephosphorylation experiments, 60 μg of protein extract was treated with 50 units of calf alkaline phosphatase (New England BioLabs) in buffer provided by the

Requests for reprints: Peter H. King, University of Alabama at Birmingham Department of Neurology, SC 200, 1530 3rd Avenue South, Birmingham, AL 35294-0017. Phone: 205-975-8116; Fax: 205-996-7255; E-mail: pking@uab.edu.

doi:10.1158/0008-5472.CAN-07-2751

manufacturer. After a 2-h incubation at 37°C, extracts were resolved on a 10% SDS gel. For kinase inhibitor assays, U251MG and U251MG tet-on cells were seeded in six-well plates at a density of 4×10^4 cells per well. The following day, U251MG cells were treated with 5 μmol/L SB203580 (Calbiochem), 10 μmol/L PD98059 (Calbiochem), or DMSO vehicle. Cells were harvested with M-Per lysis buffer (Pierce Endogen) after 24 h. TTP#6 cells were treated with SB203580 (5 μmol/L), PD98059 (10 μmol/L), or DMSO for 2 h, induced with doxycycline (1.5 μg/mL), and harvested after 6 h. Fifty micrograms of extract were analyzed by Western blot. For ELISA analysis, 3×10^4 cells were seeded in 48-well plates and stimulated with doxycycline in the presence or absence of TNF-α (10 ng/mL). Secreted IL-8 or VEGF was quantified in growth media by ELISA using commercial kits (R&D Systems). Total extract was prepared from the cells and quantified using the bicinchoninic acid kit (Pierce Endogen). All ELISA values were normalized to total protein as described previously (7). The following antibodies were used: TTP (Abcam), FLAG and tubulin (Sigma), HuR, TIA-1,and TIAR (Santa Cruz Biotechnology).

RNA kinetics, UV cross-linking, and immunoprecipitation. For RNA kinetic analysis, we used actinomycin D and assessed IL-8 and VEGF mRNA expression by quantitative reverse transcription–PCR (qRT-PCR; ref. 7). Cells were induced with doxycycline for 24 h followed by TNF-α (10 ng/mL) for 24 h. Degradation plots were generated by calculating the percentage RNA remaining at each time point after the addition of actinomycin D. UV cross-linking and immunoprecipitation were performed as described elsewhere (7). For quantification of endogenous RNA binding, cells were treated with doxycycline at a dose of 1.0 μg/mL and then stimulated with TNF-α (10 ng/mL). Cytoplasmic extract (200 μg) was equally divided into four aliquots and immunoprecipitated with the corresponding antibody using methods described elsewhere (8). RNA was extracted from beads and supernatants using the RNeasy kit (Qiagen) and then analyzed by qRT-PCR for target RNA expression.

Cell proliferation, viability, and apoptosis. Cells were seeded at density of 5×10^3 in 96-well plates overnight and induced with doxycycline for 48 h with 10% fetal bovine serum. For some cells, TNF-α (10 ng/mL) was added after 24 h of doxycycline treatment. Cells were lysed, and proliferation was assessed using the ViaLight Plus kit (CAMBREX). Luminescence was measured in a Spectrafluor plus machine (Tecan). For viability assays, TTP was induced at various doses of doxycycline for 24 h and then for additional time intervals (24–48 h). Cell viability was assessed by Trypan Blue exclusion. Assays were done in triplicate in two independent experiments. Apoptosis was assessed by fluorescence immunohistochemistry of fixed cells for cleaved caspase-3. Cells were grown on chamber slides, stimulated with doxycycline or vehicle, fixed in 4% paraformaldehyde for 20 min, and washed in PBS. After incubation for 15 min in blocking buffer (PBSBB; 1% bovine serum albumin, 0.2% evaporated milk, 0.3% Triton X-100 in PBS), primary antibody (rabbit anticleaved caspase-3; Cell Signaling Technologies) was added at 1:500 in PBSBB without triton X-100 overnight at 4°C. After PBS wash, horseradish peroxidase–conjugated donkey anti-rabbit IgG secondary antibody (Jackson Immunoresearch Laboratories) was added at 1:3,000 in PBSBB without triton X-100 for 1 h at room temperature followed by PBS wash. Antibody staining was detected using a tyramide signal amplification system with Cy3-conjugated tyramide (1:1,500, 30 min, room temperature) according to manufacturer's instructions (Perkin-Elmer), followed by PBS wash. Nuclei were subsequently counterstained with *bis*-benzimide (2 μg/mL; Hoechst 33,258; Sigma) for 10 min, followed by PBS wash. Slides were coverslipped in a 1:1 mixture of PBS and glycerol. Cells were examined with a Zeiss Axioskop inverted microscope equipped with epifluorescence. Images were captured from each well using Axiovision software using a constant exposure time for each image. Numbers of cleaved caspase-3–positive cells were counted from five images captured randomly from each well and were expressed as a percentage of total cell number (nuclei) for each well. Percentages of cleaved caspase-3–positive cells were averaged together for each doxycycline dose.

Statistics. For comparison of RNA and ELISA expression levels, a Mann-Whitney test was used. An unpaired, two-tailed Student's *t* test was used for analysis of cell proliferation, viability, and cleaved caspase-3 activity.

Results

Expression of TTP in glioma cells. In our previous work, we have shown that gliomas overexpress the RNA stabilizer HuR and have active RNA stabilization pathways (6, 7). Because TTP is a negative regulator of adenine and uridine-rich mRNAs, including some of the same growth factor mRNAs stabilized by HuR, we postulated that this protein would be down-regulated or absent in glioma cells. We analyzed different glioma cell lines and detected consistent expression of TTP but at variable levels (Fig. 1*A*). Whereas the predicted molecular weight of TTP is ~34 kDa, we observed two to five bands between 37 and 50 kDa. This finding is consistent with prior reports indicating altered electrophoresis of this protein because of phosphorylation (9–11). The slower migrating forms were most prominent in U251MG and U87 cells (lanes 1–4), and treatment with TNF-α did not alter their expression (lanes 1 and 3 versus lanes 2 and 4). These upper bands were minimally detectable in other glioma cell lines (lanes 5–11). The lower bands, which most closely match the predicted molecular weight (12), were observed in all cell lines, although faintly in D37 cells. Next, we stably transfected a FLAG-TTP plasmid into U251MG tet-on cells using methods previously published from this laboratory (7). One clone, TTP#6, was further analyzed by Western blot and a FLAG antibody (Fig. 1*B*). By varying the dose of doxycycline, we observed differential expression of the transgene up to 3.0 μg/mL doxycycline. Throughout dose escalation, slower-migrating phosphorylated forms predominated (most noticeable at doses of >0.5 μg/mL). To confirm that these bands reflected phosphorylated forms of TTP, we treated the extracts with calf intestinal alkaline phosphatase. Western blot with an anti-FLAG antibody showed loss of upper bands at each dose of doxycycline, confirming that the ectopic protein was phosphorylated (Fig. 1*B, bottom*). Because endogenous TTP expression is induced with serum (11), we tested the level of induction when the cells were exposed to serum concentrations ranging from 0% to 10% (Fig. 1*C*). Western blot with a FLAG antibody indicated weak expression of TTP in serum-deprived conditions, which became progressively stronger with higher concentrations of serum. Furthermore, the phosphorylated forms did not appear until serum was added, which is consistent with prior findings in other cell systems (9, 11). In the presence of TNF-α, expression of TTP (including the phosphorylated forms) was considerably more robust at low concentrations of serum. We next treated TTP#6 cells with the p38/mitogen-activated protein kinase (MAPK) inhibitor SB203580 and the extracellular signal-regulated kinase 1/2 (ERK1/2) inhibitor PD184352 to determine the contribution of these kinases to TTP phosphorylation. Cells were treated with inhibitor or control for 2 h before induction with doxycycline. Extracts were prepared 6 h after doxycycline treatment and analyzed by Western blot using a FLAG antibody (Fig. 1*D*). With SB203580, there was near abrogation of the upper band(s) compared with the control lane, whereas with PD184352, there was a modest diminution. We then treated wild-type U251MG cells with SB203580 or PD184352 for 24 h and found a loss of upper bands with SB203580 but not PD184352 using a TTP antibody. Thus, p38/MAPK plays a major role in phosphorylation of TTP in U251MG cells.

TTP destabilizes growth factor mRNAs in malignant glioma cells. We next analyzed the RNA kinetics of IL-8 and VEGF, two angiogenic growth factor mRNAs that are targets of mRNA stabilization in gliomas (6, 7, 13, 14). Based on our previous work,

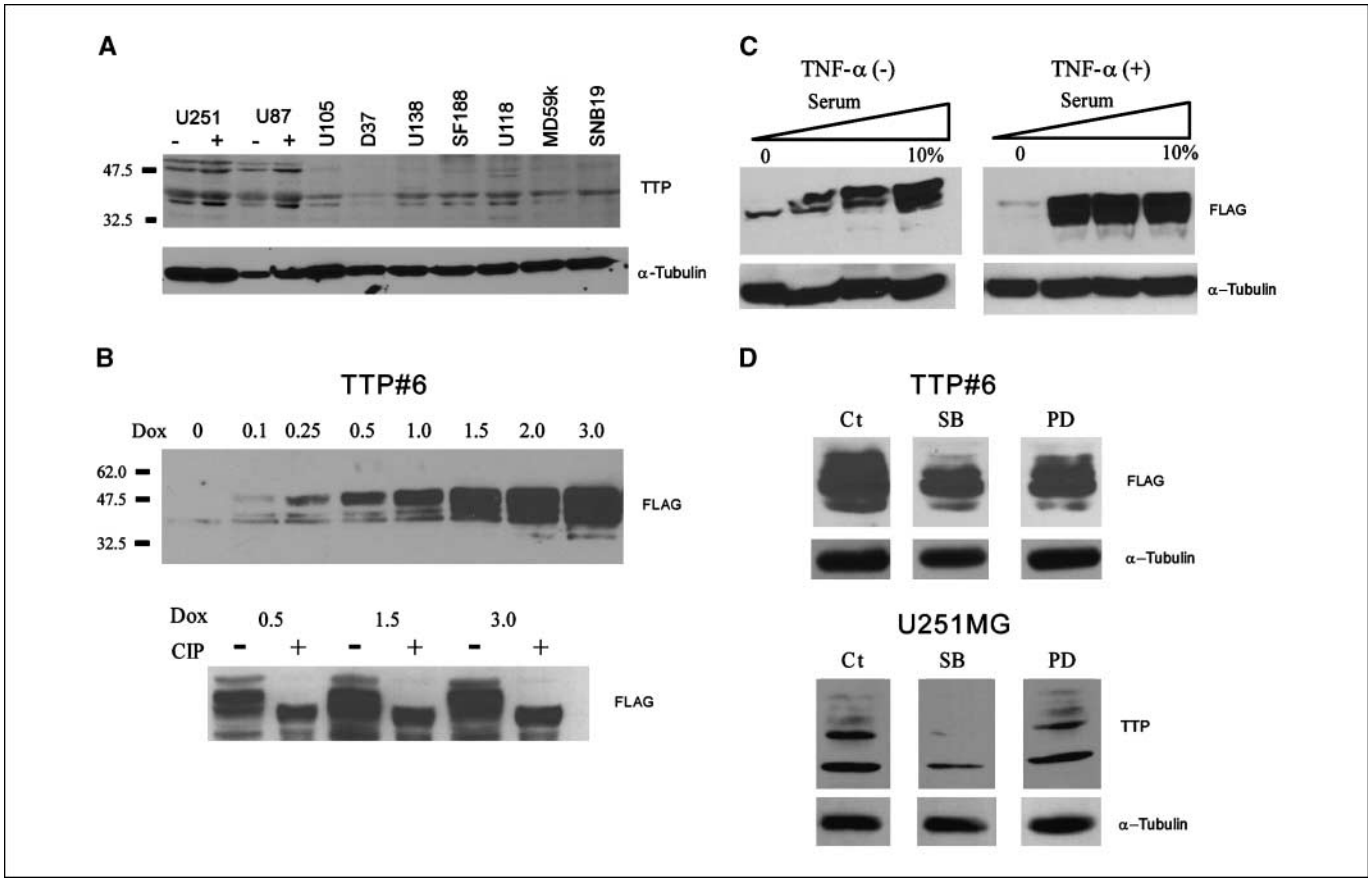

Figure 1. Western blot analysis of TTP expression in glioma cell lines. Antibodies used are shown to the right of each blot. *A,* various glioma cell lines using an anti-TTP antibody; (+), stimulated with TNF-α for 24 h; (−), no stimulation. *B, top,* blot of U251MG tet-on clone expressing FLAG-TTP (TTP#6) treated with varying doses of doxycycline (*Dox*) for 48 h to induce expression. *Bottom,* blot of extracts from TTP#6 cells treated with calf intestinal alkaline phosphatase (*CIP*). *C,* TTP#6 cells grown in the presence of varying amounts of fetal bovine serum (0%, 2.5%, 5.0%, 10.0%) during induction with doxycycline for 24 h. *D, top,* blot of TTP#6 cells treated for 2 h before doxycycline stimulation with the following kinase inhibitors: SB203580 (*SB*) at 5 μmol/L, PD184352 (*PD*) at 10 μmol/L, or DMSO control (*Ct*). Cells were harvested 6 h after doxycycline induction. *Bottom,* blot of U251MG cells were treated with the same kinase inhibitors and concentrations for 24 h before harvesting cells.

we treated the cells with TNF-α for 24 h to induce RNA expression for measurement of decay curves (7). We observed a doxycycline dose–dependent reduction of RNA half-life with both target RNAs (Fig. 2, *top*). For IL-8, the change in half-life was striking. At baseline (no doxycycline), the half-life was >6 h, which is consistent with our previous report of TNF-α–induced RNA stabilization in this cell line (7). With escalating doses between 0.25 and 1.5 μg/mL doxycycline, however, the half-life was reduced to ~4 and 2 h, respectively. For VEGF, the half-life was reduced by 2.5-fold at a doxycycline dose of 1.5 μg/mL (from ~4.0 to 1.6 h). We did not increase the dose beyond 1.5 μg/mL despite greater induction of the transgene because we have observed an effect of doxycycline on RNA kinetics in the parent U251 tet-on cell line at doses higher than 2.0 μg/mL (data not shown). The effect of this half-life reduction on RNA expression was then assessed. We found a dose-dependent decline in RNA levels compared with baseline (Fig. 2, *bottom*). The negative effect of TTP was greater for VEGF, where a dose of 0.25 μg/mL of doxycycline produced a significant decline in RNA levels compared with baseline. At the highest dose, there was a 74% decline in RNA levels ($P < 0.01$). For IL-8, a significant drop in RNA level was not observed until a doxycycline dose of 0.5 μg/mL. Part of this discrepancy may be due to the differential induction of RNAs with TNF-α stimulation. For IL-8, there was a robust induction (on average, 70-fold) versus no significant induction for VEGF in the presence or absence of doxycycline (data not shown). We have also observed this difference in U251MG cells as well (7). Thus, the potent transcriptional effect of TNF-α on IL-8 may, in part, compensate for the decline in RNA half-life.

TTP binds to IL-8 and VEGF mRNA. We next determined whether destabilization of the target mRNA was linked to binding with ectopic FLAG-TTP. Although TIS11b, a homologue of TTP, has been shown to bind VEGF 3′ UTR (15), binding to IL-8 3′ UTR has not been described previously. Both 3′ UTRs have several optimal nonamers (UUAUUUAUU) for TTP binding in the context of an adenine and uridine-rich 3′ UTR (Fig. 3*A*; ref. 16). We performed UV cross-linking (UVX) with TTP#6 extracts and radiolabeled IL-8 and VEGF 3′ UTR probes (gels in Fig. 3*B* and *C*). The location of the probes is shown in Fig. 3*A*. Analysis of the cross-linked extract revealed a spectrum of bands ranging from 34 to 80 kDa (UVX lane). We observed a hyper-intense band signal in the size range expected for FLAG-TTP based on Western analysis (Fig. 1*B*). We then performed immunoprecipitation of the UVX extract with a FLAG antibody and detected the TTP fusion protein in the same size range for both 3′ UTR probes. Immunoprecipitation with the TTP antibody revealed a similar cluster of bands. Cross-linked endogenous HuR was also immunoprecipitated, indicating that the

two RBPs bind to similar loci within the 3′ UTR (7, 8). Interestingly, a second, diffuse band of slower mobility was observed in immunoprecipitation of HuR with the VEGF probe, suggesting either the presence of a modified form of HuR or coprecipitation of another RBP. As UVX of cell extracts produces only qualitative assessment of RNA binding, we determined quantitatively the endogenous binding of mRNA targets to ectopic FLAG-TTP. Cytoplasmic extracts from cells stimulated with TNF-α were prepared under nondenaturing conditions and subjected to immunoprecipitation without cross-linking. RNA was eluted and quantified by qRT-PCR for IL-8 and VEGF mRNA expression using the same pellet and supernatant (graphs in Fig. 3*B* and *C*). For additional controls, we analyzed two other ARE-binding proteins, TIA-1 and TIAR, both of which bind to similar loci in the 3′ UTR (17). Without doxycycline stimulation, there was a relative increase in recovery of VEGF mRNA with the HuR antibody compared with FLAG, TIAR, or TIA1. For IL-8 mRNA, there were only minimal differences. Some recovery was observed with the FLAG antibody consistent with basal expression of the tet-on system (18). This finding is consistent with our previous observations indicating an RNA stabilizing effect of TNF-α stimulation (7). After doxycycline induction of FLAG-TTP, there was an increase in RNA recovery for both targets (3.5-fold for IL-8 and 6-fold for VEGF). HuR binding, on the other hand, declined by 35-fold for VEGF and 2-fold for IL-8. For TIA-1, there was modest recovery of RNA under basal conditions which did not change substantially after doxycycline treatment. TIAR, however, showed little (IL-8) or no (VEGF) recovery regardless of doxycycline treatment.

Overexpression of TTP reduces IL-8 and VEGF production. We next sought to determine whether FLAG-TTP expression negatively affected protein expression. We examined TTP#6 and U251MG tet-on cells treated with and without TNF-α at varying doses of doxycycline (Fig. 4). After normalization to total protein, ELISA values were expressed as a percentage of the average value at doxycycline dose of 0. Under basal conditions, there was a dose-dependent reduction of IL-8 and VEGF levels in the supernatant of TTP#6 cells. At the highest dose of doxycycline (2.0 μg/mL), there was a 3.2-fold decline in IL-8 and a 4.2-fold decline in VEGF protein levels compared with control cells. At each doxycycline dose, there was a significant difference between TTP#6 and control cells for both proteins, even with the negative effect of doxycycline on IL-8 production in control cells. With TNF-α stimulation, there continued to be a significant doxycycline dose–dependent decline in VEGF production, with an 80% reduction at 2.0 μg/mL (7.2-fold decline compared with control cells). Interestingly, IL-8 showed no significant drop compared with control at all doses of doxycycline.

TTP overexpression is toxic to glioma cells. Because VEGF and IL-8 are important angiogenic growth factors in glioma tumor progression (19–21), we wanted to determine whether expression of TTP adversely affected cell growth and proliferation. Using a luciferase-based assay, we observed a significant dose-dependent decrease in proliferation of TTP#6 versus tet-on control cells at 24 h that was substantially augmented by TNF-α (Fig. 5*A*). We then examined cell viability up to 48 h using a Trypan Blue exclusion assay (Fig. 5*B*). In the initial 24 h, there was no reduction in cell counts in the TTP clone; however, in the 48-h time interval, there was a significant doxycycline dose–dependent reduction in viable cells. Control cells showed no change in viability regardless of doxycycline dose. Thus, TTP expression exerted a negative effect on both proliferation and cell survival. To determine if overexpression of TTP induced apoptosis, cleaved caspase-3 immunohistochemistry was performed on paraformaldehyde-fixed cells. Representative fields are shown in Fig. 5*C* where only TTP#6 cells treated with doxycycline showed positive cells at 48 h. Quantitative assessment

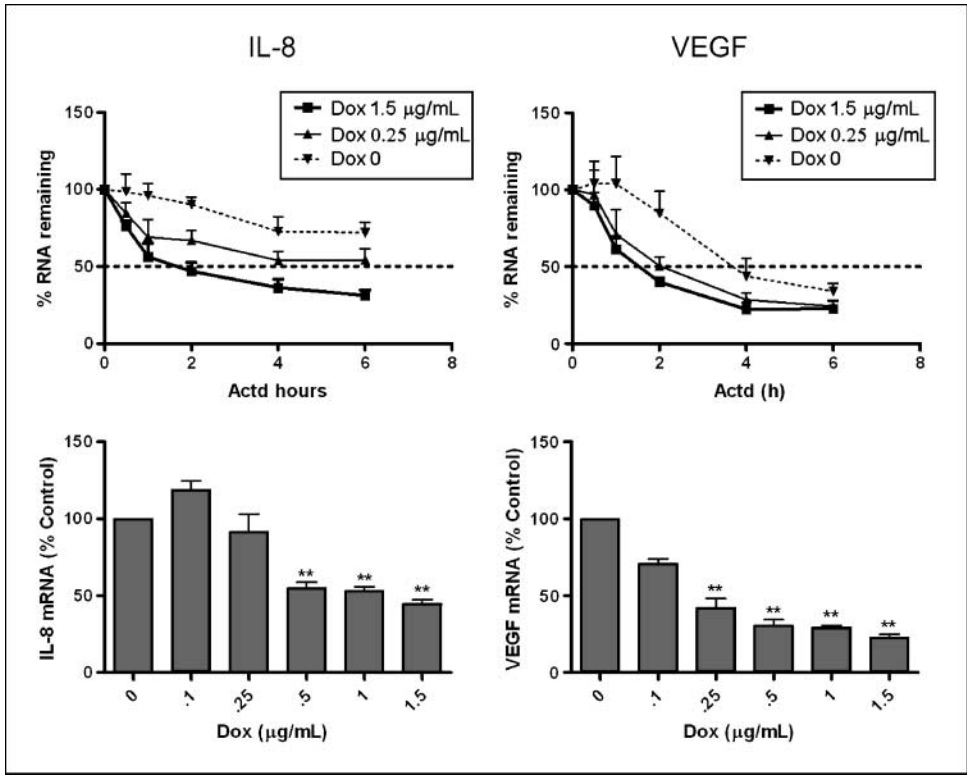

Figure 2. Kinetics and RNA expression of IL-8 and VEGF mRNA in U251MG cells expressing a doxycycline-inducible TTP transgene. *Top,* RNA decay curves after the addition of actinomycin D (*ActD*) at the doses of doxycycline indicated (see Materials and Methods). *Bottom,* total RNA levels measured after treatment of the cells with the indicated dose of doxycycline. **, $P < 0.01$.

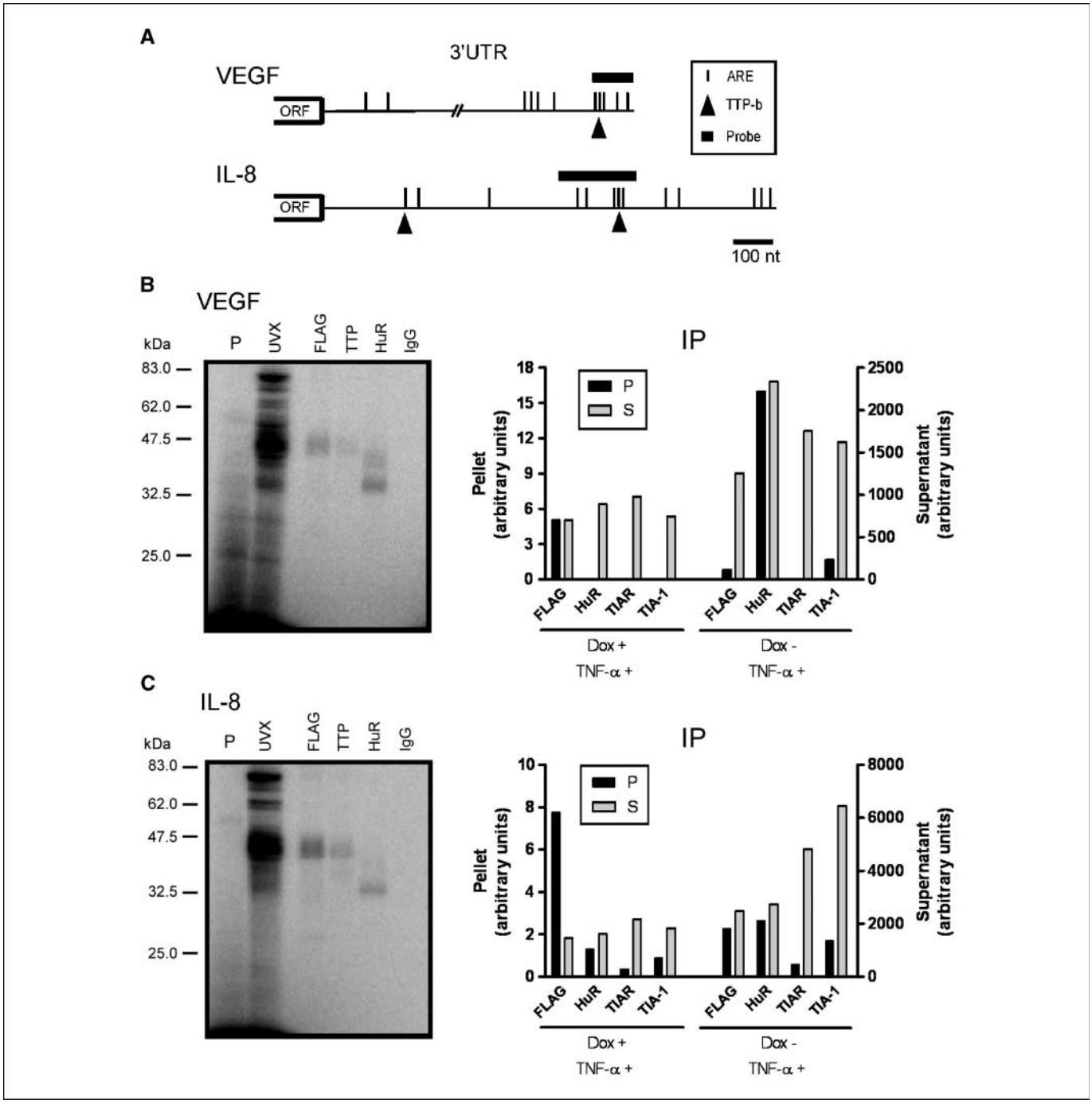

Figure 3. RNA-binding patterns of IL-8 and VEGF in U251 TTP#6 cells. *A,* schematic diagram of IL-8 and VEGF 3′ UTRs indicating the location of the ARE, optimal TTP-binding nonamer (*TTP-b*) and probes used for UVX. *B, left,* phosphorylated image of UV cross-linked extract with the VEGF 3′ UTR probe. *P,* probe alone. The subsequent lanes are immunoprecipitations of the cross-linked extract with FLAG, TTP, HuR, and IgG antibodies. *Right,* qRT-PCR quantification of endogenous VEGF mRNA recovered (expressed as arbitrary units) after immunoprecipitation of various RNA-binding proteins using the antibodies shown. *P,* pellet; *S,* supernatant. *C,* same as *B*, except IL-8 3′ UTR probe and mRNA were analyzed.

of immunoreactivity showed a dose-dependent and significant increase in cleaved caspase-3 positivity for TTP#6 compared with control (Fig. 5*D*). Virtually no positive cells were observed with TTP#6 cells in the absence of doxycycline. These results suggest that the doxycycline-induced expression of TTP induces an apoptotic program of cell death in U251MG cells.

TTP is hyperphosphorylated in primary malignant gliomas. The observed deleterious effects of TTP expression on angiogenic growth factor expression and survival in our glioma clone would not be compatible with the robust growth properties of malignant gliomas. We therefore investigated TTP expression patterns in highly malignant and infiltrative GBM tumors, more indolent and low-infiltrative pilocytic astrocytomas, or nonneoplastic astrogliotic tissue (Fig. 6). TTP expression was readily detected in all tissues, with GBM and pilocytic astrocytoma surprisingly showing a stronger intensity of bands than astrogliotic samples. However,

in both GBM and pilocytic astrocytoma, hyperphosphorylated forms of TTP predominated. Some of the bands were greater than the 47.5-kDa molecular marker, similar to what we observed in glioma cell lines and the FLAG-TTP clone. In contrast, astrogliotic tissues showed a predominance of the lesser phosphorylated forms. Thus, it seems that hyperphosphorylated forms predominate in malignant tumors, although there was not an obvious difference between the lower grade pilocytic astrocytoma and GBM.

Discussion

We have shown that ectopic expression of TTP led to a concentration-dependent destabilization and down-regulation of IL-8 and VEGF mRNAs in malignant glioma cells. This destabilization was linked to increased binding of TTP to these target mRNAs. At the cellular level, there was a dose-dependent decline in proliferation followed by loss of cell viability and apoptosis in the ensuing 48 h. Analysis of primary gliomas and benign astrogliotic tissues indicated ubiquitous expression of TTP. In malignant glioma tumors, however, there was prominent phosphorylation of TTP compared with benign tissues. We postulate that hyperphosphorylation, mediated by p38/MAPK, keeps this RBP in check in malignant glioma, thereby providing a permissive environment for RNA stabilization and up-regulation of IL-8, VEGF, and potentially other mRNAs encoding growth-associated and survival-associated proteins.

Malignant gliomas are highly aggressive tumors characterized by rapid growth and poor prognosis (22). Growth factor signaling for gliomas, triggered by both autocrine and paracrine pathways, remains unchecked, allowing for rapid proliferation and angiogenesis. Gliomas rely on production of key angiogenic growth factors, such as VEGF and IL-8, to drive this phenotype (2, 22, 23). Growth factor signaling in normal states is typically attenuated by coordinated activation of genes that negatively regulate mediators of the signaling cascade (24). RNA degradation represents one control point, and TTP induction has recently been linked to this attenuation (24). In gliomas, we have shown here and previously that there is a shift away from mRNA degradation toward stabilization (6, 7). Despite endogenous TTP expression in glioma cells, there was complete stabilization of IL-8 (>6 h) and a prolongation of VEGF half-life ($\sim$ 4 h) when the TTP transgene was suppressed (Fig. 2). Determinants of RNA stability are complex because RNA destabilizers, such as TTP, AUF1, and KSRP, overlap in expression with the RNA stabilizer HuR (25, 26). We have observed KSRP and AUF1 expression in glioma cell lines, including the one used in this study (data not shown). Several possible conditions may contribute to the overall stability of target mRNAs. First, RNA binding may be competitive and relate to the amount of RBP available for binding (26–30). In one study, when HuR was ectopically expressed in NIH 3T3 cells, a major change in the EMSA band pattern was observed, with loss of most bands except the complex containing HuR (31). Likewise, cotransfection of TTP antagonized the RNA stabilizing effect of transfected HuR (30). These findings suggest that high amounts of one RBP can tip the balance of RNA stability through displacement of other RBPs. This possibility is pertinent to our study as we observed a reversal of IL-8 and VEGF mRNA stabilization when ectopic TTP was

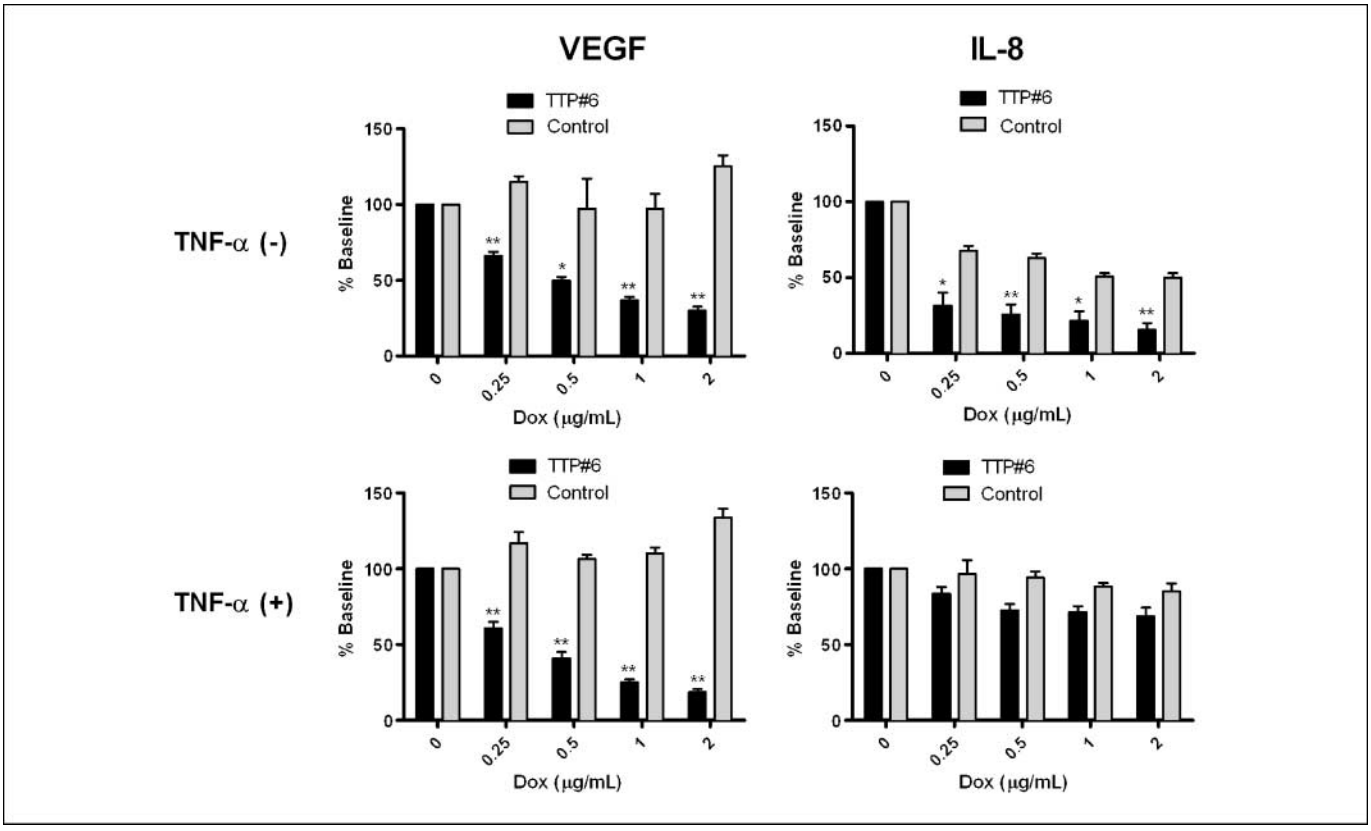

Figure 4. ELISA analysis of VEGF and IL-8 expression in TTP#6 clone. Cells were induced with doxycycline for 24 h and then stimulated with TNF-α or vehicle (PBS) for an additional 24 h. Proteins were assayed from growth medium, normalized to total cellular protein in the well, and expressed as a percentage ($\pm$SE) of the average value at baseline (doxycycline, 0). U251MG tet-on cells were used as a control. Results represent an average of three different experiments, each with duplicate or triplicate measurements. *, $P < 0.05$; **, $P < 0.01$ comparing control to TTP#6 at each dose of doxycycline.

expressed at higher levels (e.g., doxycycline dose of 1.5 versus 0.25 μg/mL; Fig. 2). The relative increase in IL-8 and VEGF mRNA bound to ectopic TTP and a concomitant reduction of binding to HuR (Fig. 3*B* and *C*) suggest a competitive process of binding between HuR and TTP. These observations are supported by data from primary glioma tumors, where HuR is highly expressed in malignant glioma, and thus may outcompete other RBPs for target ARE mRNAs (7). The second possible condition is modification of the RBP to reduce RNA binding affinity and function. TTP has multiple serine residues that can be phosphorylated, creating the pattern of altered mobility on gel electrophoresis (Fig. 1; refs. 9–11, 32). Several studies have shown diminished ARE binding with TTP phosphorylation (33–35), whereas others have not (10, 12, 32). Phosphorylation also creates a novel 14-3-3 binding site that may impair TTP function by sequestering it away from cytoplasmic stress granules (32, 36–38). We observed extensive phosphorylation of endogenous and ectopically expressed TTP in U251MG cells (Fig. 1). At higher doses of doxycycline (≥1.5 μg/mL), however, there was stronger expression of unphosphorylated forms (Fig. 1*B*), which may explain the dose effect of RNA destabilization (Fig. 2). Interestingly, ectopic TTP expression and phosphorylation were dependent on serum in the media (Fig. 1*C*). TTP is an inducible protein, and a number of mitogens, including serum, phorbol esters, fibroblast growth factor, and platelet-derived growth factor (PDGF), are potent triggers for expression and phosphorylation (39). Serum exposure typically leads to rapid induction of TTP transcription followed by increases in protein expression. In our system, however, TTP transcriptional control elements (and even 3′ UTR elements) were not present. We were able to detect induction of FLAG-TTP RNA with doxycycline treatment in the absence of serum (not shown) yet could detect little protein (Fig. 1*C*). This discrepancy suggests that TTP expression is regulated posttranslationally in U251MG (e.g., protein stability) as observed in other cells (40).

Our tet-on system permitted analysis of phosphorylation at an early phase of TTP production, and p38/MAPK inhibition led to a loss of slower-migrating bands compared with control. In wild-type U251MG cells, all upper bands disappeared with p38/MAPK inhibition, further confirming a major role for this pathway in TTP phosphorylation. Although p38-MAPK is a major pathway for TTP phosphorylation in other cell systems, alternative kinases have been implicated, including c-Jun-NH_2-kinase, ERK, and p42 MAPK (11, 12, 40, 41). We did not observe a significant effect of ERK1/2 inhibition on phosphorylation in wild-type U251MG cells and only a modest effect on ectopic TTP. Interestingly, a recent study showed that active forms of p38/MAPK and MKK3 (an upstream activator of p38/MAPK) are significantly up-regulated in malignant gliomas and are strongly linked to tumor progression, invasiveness, and poor prognosis (42). Attenuation of TTP by p38/MAPK-induced phosphorylation would thus contribute to the malignant phenotype by creating a permissive environment for HuR-induced RNA stabilization (7, 30). In support of this hypothesis was the extensive phosphorylation of TTP observed in primary malignant glioma tumors (Fig. 6). TTP-induced mRNA destabilization led to a

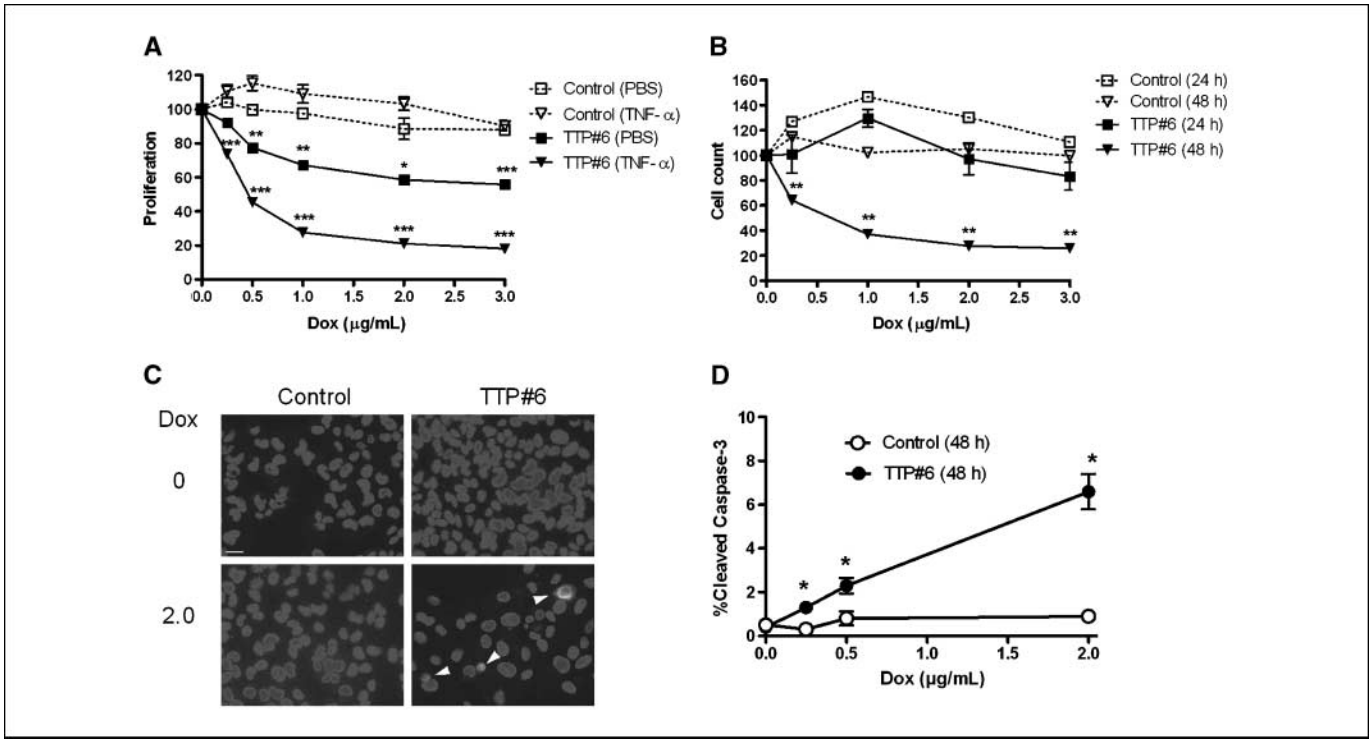

Figure 5. Proliferation and cell viability of theTTP#6 clone versus control U251 tet-on cells with varying doses of doxycycline. *A,* proliferation assay after 24 h of doxycycline treatment (see Materials and Methods) expressed as a percentage of baseline (doxycycline, 0); *bars,* SE. Some cells were treated with TNF-α for 24 h or vehicle (PBS) as indicated. *B,* cell viability determined by a Trypan Blue exclusion assay after the indicated time interval. All cell counts are expressed as a percentage of baseline (doxycycline, 0); *bars,* SE. *C,* representative fields of cleaved caspase-3 immunofluorescence for TTP#6 or control cells after doxycycline treatment for 48 h (*bar,* 20 μm). *D, points,* mean for the percentage of cleaved caspase-3–positive cells averaged together from five random fields for each doxycycline dose after 48 h; *bars,* SE (see Materials and Methods). Data for cell proliferation and viability were derived from four to six independent assays. Data for cleaved caspase-3 immunohistochemistry are representative of two independent experiments with similar results. *, $P < 0.05$; **, $P < 0.005$; ***, $P < 0.001$ comparing control to TTP#6 at each dose of doxycycline.

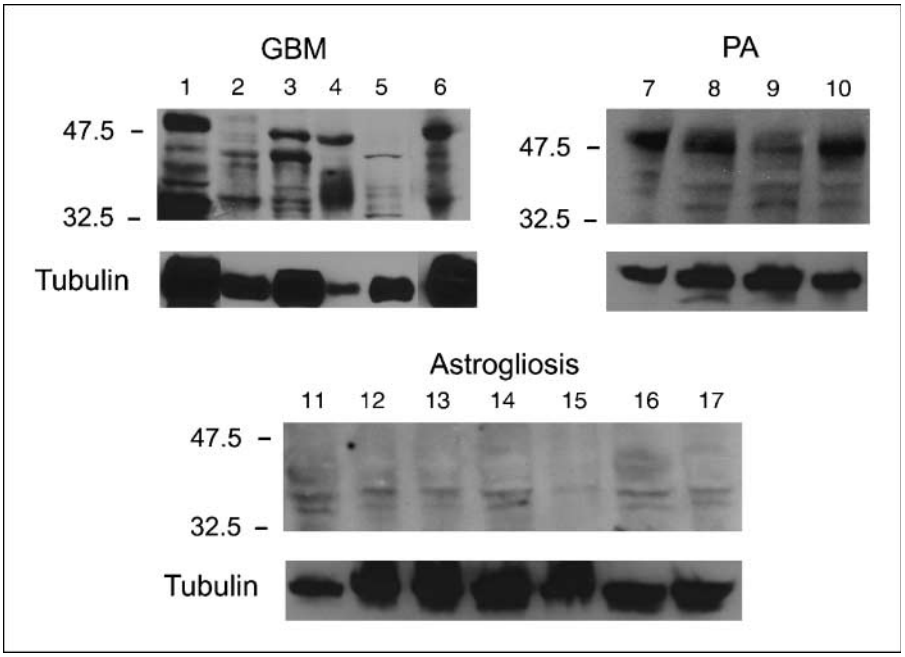

Figure 6. Western blot of six high-grade and four low-grade malignant glioma tumors and seven samples from benign astrogliotic (normal brain) tissues using a TTP antibody. The blots were stripped and probed with an α-tubulin antibody as shown. *Lanes 1–6,* GBM samples; *lanes 7–10,* pilocytic astrocytoma (*PA*) samples; *lanes 11–17,* benign astrogliotic tissue samples.

significant and dose-dependent reduction in levels of IL-8 and VEGF mRNA (Fig. 2). In contrast to VEGF, the negative effect of TTP on IL-8 expression was blunted after TNF-α stimulation. In fact, there was no substantial change in IL-8 protein production (Fig. 4). This cytokine is a potent inducer of IL-8 in glioma cells (3) and suggests that increased transcriptional activity can compensate for loss of RNA stabilization. It also indicates a selective vulnerability of certain mRNA targets (e.g., VEGF in this case) to RNA destabilization when there is little compensatory increase in transcription.

The early inhibitory effect of TTP overexpression on proliferation and the later-onset apoptotic effect was exquisitely dependent on the level of TTP expression and duration of exposure. Even at high doses of doxycycline stimulation, there was no loss of cell viability at 24 h (Fig. 5). This delay in apoptotic cell death is consistent with previous observations in NIH3T3 cells transfected with TTP, where maximal cell death was not observed until 48 h (43). TNF-α augmented the negative effect on proliferation in the initial 24 h consistent with prior observations in nonglioma cell lines (43, 44). Glioma cells, including the ones used in this study, are often resistant to the antiproliferative effects of TNF-α (45). So how does TTP induce cytotoxicity in glioma cells? Clearly IL-8 and VEGF mRNAs were destabilized in the presence of TTP with a significant reduction in expression. Both factors have been linked to glioma proliferation, angiogenesis, and invasion through paracrine and possibly autocrine pathways (2, 3). Down-regulation of IL-8 expression in malignant glioma cells, including U251, has been shown to inhibit proliferation and invasion *in vitro*, although tumor cells *in vivo* do not seem to express IL-8 receptors (2, 3). Whereas many glioma cells express VEGF receptors (46), down-regulation of VEGF or neutralization of the receptor failed to show a significant effect on proliferation (46). Thus, TTP may induce cytotoxicity by negatively regulating other ARE mRNA(s) important for glioma survival and proliferation. A Genbank database analysis indicates that up to 8% of human mRNAs contain AREs (47). Epidermal growth factor receptor and PDGF are components of two critical autocrine growth pathways in gliomas, and both have AREs in the 3′ UTR (22, 47). Disruption of these autocrine loops may impair tumor growth and progression. A precedent for this possibility has been observed in a mast cell tumor model where TTP produced an antioncogenic effect by blocking a critical autocrine loop dependent on IL-3 (which contains AREs in the 3′ UTR; ref. 48). Thus, TTP-induced destabilization could have a synergistically negative effect on glioma proliferation by down-regulating effectors of multiple growth pathways. In that respect, targeting TTP overexpression to glioma cells may produce a therapeutic effect, particularly if critical serine residues are altered to prevent deactivation through phosphorylation.

Acknowledgments

Received 7/19/2007; revised 10/25/2007; accepted 11/20/2007.

Grant support: Brain Tumor Specialized Programs of Research Excellence grant P50 CA097247 (G.Y. Gillespie) and a supplement to Brain Tumor Specialized Programs of Research Excellence P50 CA097247-04S1 (E.A. Shacka) awarded to University of Alabama at Birmingham by NIH and Merit Review award from Department of Veterans Affairs (P.H. King).

The costs of publication of this article were defrayed in part by the payment of page charges. This article must therefore be hereby marked *advertisement* in accordance with 18 U.S.C. Section 1734 solely to indicate this fact.

References

1. Dunn IF, Heese O, Black PM. Growth factors in glioma angiogenesis: FGFs, PDGF, EFG, and TGFs. J Neurooncol 2000;50:121–37.
2. Machein MR, Plate KH. VEGF in brain tumors. J Neurooncol 2000;50:109–20.
3. Brat DJ, Bellail AC, Van Meir EG. The role of interleukin-8 and its receptors in gliomagenesis and tumoral angiogenesis. Neurooncology 2005;7:122–33.
4. Mukhopadhyay D, Datta K. Multiple regulatory pathways of vascular permeability factor/vascular endothelial growth factor (VPF/VEGF) expression in tumors. Semin Cancer Biol 2004;14:123–30.
5. Audic Y, Hartley RS. Post-transcriptional regulation in cancer. Biol Cell 2004;96:479–98.
6. Nabors LB, Gillespie GY, Harkins L, King PH. HuR, an RNA stability factor, is expressed in malignant brain tumors and binds to adenine and uridine-rich elements within the 3′ untranslated regions of cytokine and angiogenic factor mRNAs. Cancer Res 2001;61:2154–61.

7. Nabors LB, Suswam E, Huang Y, Yang X, Johnson MJ, King PH. Tumor necrosis factor-a induces angiogenic factor up-regulation in malignant glioma cells: a role for RNA stabilization and HuR. Cancer Res 2003;63: 4181–7.
8. Suswam EA, Nabors LB, Huang Y, Yang X, King PH. IL-1b induces stabilization of IL-8 mRNA in malignant breast cancer cells via the 3′ untranslated region: involvement of divergent RNA-binding factors HuR, KSRP and TIAR. Int J Cancer 2005;113:911–9.
9. Cao H, Tuttle JS, Blackshear PJ. Immunological Characterization of tristetraprolin as a low abundance, inducible, stable cytosolic protein. J Biol Chem 2004;279: 21489–99.
10. Cao H, Deterding LJ, Venable JD, et al. Identification of the anti-inflammatory protein tristetraprolin as a hyperphosphorylated protein by mass spectrometry and site-directed mutagenesis. Biochem J 2006;394: 285–97.
11. Taylor GA, Thompson MJ, Lai WS, Blackshear PJ. Phosphorylation of tristetraprolin, a potential zinc finger transcription factor, by mitogen stimulation in intact cells and by mitogen-activated protein kinase *in vitro*. J Biol Chem 1995;270:13341–7.
12. Cao H, Dzineku F, Blackshear PJ. Expression and purification of recombinant tristetraprolin that can bind to tumor necrosis factor-a mRNA and serve as a substrate for mitogen-activated protein kinases. Arch Biochem Biophys 2003;412:106–20.
13. Damert A, Machein M, Breier G, et al. Up-regulation of vascular endothelial growth factor expression in a rat glioma is conferred by two distinct mechanisms. Cancer Res 1997;57:3860–4.
14. Ikeda E, Achen MG, Breier G, Risau W. Hypoxia-induced transcriptional activation and increased mRNA stability of vascular endothelial growth factor in C6 glioma cells. J Biol Chem 1995;270:19761–6.
15. Ciais D, Cherradi N, Bailly S, et al. Destabilization of vascular endothelial growth factor mRNA by the zinc-finger protein TIS11b. Oncogene 2004;23:8673–80.
16. Blackshear PJ, Lai WS, Kennington EA, et al. Characteristics of the interaction of a synthetic human tristetraprolin tandem zinc finger peptide with AU-rich element-containing RNA substrates. J Biol Chem 2003; 278:19947–55.
17. Forch P, Valcarcel J. Molecular mechanisms of gene expression regulation by the apoptosis-promoting protein TIA-1. Apoptosis 2001;6:463–8.
18. Meyer-Ficca ML, Meyer RG, Kaiser H, Brack AR, Kandolf R, Kupper J-H. Comparative analysis of inducible expression systems in transient transfection studies. Anal Biochem 2004;334:9–19.
19. Bethea JR, Gillespie GY, Chung IY, Benveniste EN. Tumor necrosis factor production and receptor expression by a human malignant glioma cell line, D54-MG. J Neuroimmunol 1990;30:1–13.
20. Steiner H-H, Karcher S, Mueller MM, Nalbantis E, Kunze S, Herold-Mende C. Autocrine pathways of the vascular endothelial growth factor (VEGF) in glioblastoma multiforme: clinical relevance of radiation-induced increase of VEGF levels. J Neurooncol 2004;66: 129–38.
21. Aggarwal BB, Schwarz L, Hogan ME, Rando RF. Triple helix-forming oligodeoxyribonucleotides targeted to the human tumor necrosis factor (TNF) gene inhibit TNF production and block the TNF-dependent growth of human glioblastoma tumor cells. Cancer Res 1996;56: 5156–64.
22. Maher EA, Furnari FB, Bachoo RM, et al. Malignant glioma: genetics and biology of a grave matter. Genes Dev 2001;15:1311–33.
23. Webb CP, Vande Woude GF. Genes that regulate metastasis and angiogenesis. J Neurooncol 2000;50:71–87.
24. Amit I, Citri A, Shay T, et al. A module of negative feedback regulators defines growth factor signaling. Nat Genet 2007;39:503–12.
25. Lu J-Y, Schneider RJ. Tissue distribution of AU-rich mRNA-binding proteins involved in regulation of mRNA decay. J Biol Chem 2004;279:12974–9.
26. Barreau C, Paillard L, Osborne HB. AU-rich elements and associated factors: are there unifying principles? Nucleic Acids Res 2006;33:7138–50.
27. Linker K, Pautz A, Fechir M, Hubrich T, Greeve J, Kleinert H. Involvement of KSRP in the post-transcriptional regulation of human iNOS expression-complex interplay of KSRP with TTP and HuR. Nucleic Acids Res 2005;33:4813–27.
28. Lal A, Mazan-Mamczarz K, Kawai T, Yang X, Martindale JL, Gorospe M. Concurrent versus individual binding of HuR and AUF1 to common labile target mRNAs. EMBO J 2004;23:3092–102.
29. Raineri I, Wegmueller D, Gross B, Certa U, Moroni C. Roles of AUF1 isoforms, HuR and BRF1 in ARE-dependent mRNA turnover studied by RNA interference. Nucleic Acids Res 2004;32:1279–88.
30. Ming X-F, Stoecklin G, Lu M, Looser R, Moroni C. Parallel and independent regulation of interleukin-3 mRNA turnover by phosphatidylinositol 3-kinase and p38 mitogen-activated protein kinase. Mol Cell Biol 2001;21:5778–89.
31. Chen C-YA, Xu N, Shyu A-B. Highly selective actions of HuR in antagonizing AU-rich element-mediated mRNA eestabilization. Mol Cell Biol 2002;22:7268–78.
32. Chrestensen CA, Schroeder MJ, Shabanowitz J, et al. MAPKAP kinase 2 phosphorylates tristetraprolin on *in vivo* sites including Ser178, a site required for 14-3-3 binding. J Biol Chem 2004;279:10176–84.
33. Carballo E, Cao H, Lai WS, Kennington EA, Campbell D, Blackshear PJ. Decreased sensitivity of tristetraprolin-deficient cells to p38 inhibitors suggests the involvement of tristetraprolin in the p38 signaling pathway. J Biol Chem 2001;276:42580–7.
34. Hitti E, Iakovleva T, Brook M, et al. Mitogen-activated protein kinase-activated protein kinase 2 regulates tumor necrosis factor mRNA stability and translation mainly by altering tristetraprolin expression, stability, and binding to adenine/uridine-rich element. Mol Cell Biol 2006;26:2399–407.
35. Chen Y-L, Huang Y-L, Lin N-Y, Chen H-C, Chiu W-C, Chang C-J. Differential regulation of ARE-mediated TNFa and IL-1b mRNA stability by lipopolysaccharide in RAW264.7 cells. Biochem Biophys Res Commun 2006; 346:160–8.
36. Stoecklin G, Stubbs T, Kedersha N, et al. MK2-induced tristetraprolin: 14-3-3 complexes prevent stress granule association and ARE-mRNA decay. EMBO J 2004;23: 1313–24.
37. Marderosian M, Sharma A, Funk AP, et al. Tristetraprolin regulates cyclin D1 and c-Myc mRNA stability in response to rapamycin in an Akt-dependent manner via p38 MAPK signaling. Oncogene 2006;25:6277–90.
38. Anderson P, Kedersha N. RNA granules. J Cell Biol 2006;172:803–8.
39. Blackshear PJ. Tristetraprolin and other CCCH tandem zinc-finger proteins in the regulation of mRNA turnover. Biochem Soc Trans 2002;30:945–52.
40. Brook M, Tchen CR, Santalucia T, et al. Posttranslational regulation of tristetraprolin subcellular localization and protein stability by p38 mitogen-activated protein kinase and extracellular signal-regulated kinase pathways. Mol Cell Biol 2006;26:2408–18.
41. Dean JL, Sully G, Clark AR, Saklatvala J. The involvement of AU-rich element-binding proteins in p38 mitogen-activated protein kinase pathway-mediated mRNA stabilisation. Cell Signal 2004;16:1113–21.
42. Demuth T, Reavie LB, Rennert JL, et al. MAP-ing glioma invasion: mitogen-activated protein kinase kinase 3 and p38 drive glioma invasion and progression and predict patient survival. Mol Cancer Ther 2007;6: 1212–22.
43. Johnson BA, Geha M, Blackwell TK. Similar but distinct effects of the tristetraprolin/TIS11 immediate-early proteins on cell survival. Oncogene 2000;19:1657–64.
44. Johnson BA, Blackwell TK. Multiple tristetraprolin sequence domains required to induce apoptosis and modulate responses to TNF through distinct pathways. Oncogene 2002;21:4237–46.
45. Otsuka G, Nagaya T, Saito K, Mizuno M, Yoshida J, Seo H. Inhibition of nuclear factor-κB activation confers sensitivity to tumor necrosis factor-α by impairment of cell cycle progression in human glioma cells. Cancer Res 1999;59:4446–52.
46. Hong X, Jiang F, Kalkanis SN, et al. Decrease of endogenous vascular endothelial growth factor may not affect glioma cell proliferation and invasion. J Exp Ther Oncol 2007;6:219–29.
47. Bakheet T, Frevel M, Williams BRG, Greer W, Khabar KSA. ARED: human AU-rich element-containing mRNA database reveals an unexpectedly diverse functional repertoire of encoded proteins. Nucleic Acids Res 2001; 29:246–54.
48. Stoecklin G, Gross B, Ming X-F, Moroni C. A novel mechanism of tumor suppression by destabilizing AU-rich growth factor mRNA. Oncogene 2003;22:3554.